

Modelling of reciprocating and scroll compressors

Marie-Eve Duprez¹, Eric Dumont¹, Marc Frère*

Thermodynamics Department, Faculté Polytechnique de Mons, 31 bd Dolez, 7000 Mons, Belgium

Received 6 June 2006; received in revised form 14 November 2006; accepted 18 November 2006
Available online 22 December 2006

Abstract

This paper presents simple and thermodynamically realistic models of two types of compressors widely used in domestic heat pumps (reciprocating and scroll compressors). These models calculate the mass flow rate of refrigerant and the power consumption from the knowledge of operating conditions and parameters. Some of these parameters may be found in the technical datasheets of compressors whereas others are determined in such a way that the calculated mass flow rate and electrical power match those given in these datasheets.

The two models have been tested on five reciprocating compressors and five scroll compressors. This study has been limited to compressors with a maximum electrical power of 10 kW and for the following operating conditions: evaporating temperatures ranging from -20 to 15 °C and condensing temperatures ranging from 15 to 60 °C.

The average discrepancies on mass flow rate and power for reciprocating compressors are 1.10 and 1.69% (for different refrigerants: R134a, R404A, R22, R12 and R407C). For scroll compressors, the average discrepancies on mass flow rate and power are 2.42 and 1.04% (for different refrigerants: R134a, R404A, R407C and R22).

© 2006 Elsevier Ltd and IIR. All rights reserved.

Keywords: Refrigeration; Air conditioning; Modelling; Performance; Reciprocating piston; Scroll compressor; R134a; R404A; R22; R407C

Modélisation des compresseurs à piston et à spirale

Mots clés : Réfrigération ; Conditionnement d'air ; Modélisation ; Performance ; Compresseur à piston ; Compresseur à spirale ; R134a ; R404A ; R22 ; R407C

1. Introduction

Since the beginning of the 1990s, under the pressure of different laws concerning the limitation of CO₂ emissions, the heat pumps market has known a new expansion in the domestic sector.

In the year 2000, there were 5750 heat pumps sold in Germany for house heating, 2750 in Finland, 3000 in Norway (for both water and space heating), 23,000 in Sweden, 7200 in Switzerland and 7500 in France [1]. The

* Corresponding author. Tel.: +32 65 37 42 06; fax: +32 65 37 42 09.

E-mail addresses: marie-eve.duprez@fpms.ac.be (M.-E. Duprez), eric.dumont@fpms.ac.be (E. Dumont), marc.frere@fpms.ac.be (M. Frère).

¹ Tel.: +32 65 37 42 08; fax: +32 65 37 42 09.

Nomenclature

d	diameter (m)	ε	ratio between the dead space and the swept volume (–)
h	specific enthalpy (J kg^{-1})	η	efficiency
HP	high pressure (Pa)	ρ	density (kg m^{-3})
IP	intermediate pressure (Pa)		
LP	low pressure (Pa)		
m	mass (kg)		
N	compressor rotation speed (t min^{-1})	<i>Subscripts</i>	
p	pressure (Pa)	c	circulated
P	power (W)	calc	calculated
p_{vsat}	saturated vapour pressure (Pa)	cond	condensation
q_m	mass flow rate (kg s^{-1})	constr	constructor data
q_v	volume flow rate ($\text{m}^3 \text{s}^{-1}$)	d	dead space
s	specific entropy ($\text{J kg}^{-1} \text{K}^{-1}$)	el	electrical
T	temperature (K)	evap	evaporation
u	specific internal energy (J kg^{-1})	ex	exhaust
UA	global heat transfer coefficient (W K^{-1})	i	inlet of the compressor
v	specific volume ($\text{m}^3 \text{kg}^{-1}$)	iso-s	isentropic
V	volume (m^3)	pseudo-iso-s	pseudo-isentropic
W	work (J)	mecha	mechanical
Δp_{suc}	pressure drop in the suction valve (Pa)	s	swept
ΔT_{log}	log-mean difference temperature (K)	suc	suction
ΔT_{sup}	superheating (K)	w	fictitious wall

average growth in terms of the number of installed heat pumps between 1997 and 2000 is about 15% a year.

It is important to generalize the use of domestic heat pumps in order to decrease the primary energy consumption in the dwelling sector. For each heat pump project, the type of heat pump must be correctly chosen; the design and installation steps must be carried out carefully. For optimization purpose, it would be interesting to dispose a calculation tool able to simulate the behaviour of the heat pump integrated to the residence so that the energy consumption could be predicted and the design of the heat pump (and/or of the house) could be adapted in such a way that the environmental impact is minimized. This simulation tool should remain as simple as possible so that its use could be widespread.

In this aim of modelling such a complete system, it is important to have the simplest and the most accurate models of its components. The compressor is one of the main part of a heat pump as it sets its mass flow rate which governs the heat flows. It is thus the first component of the heat pump to be modelled.

The types of compressors used in domestic heat pumps are usually the reciprocating and scroll ones. Reciprocating compressors are mainly used as far as low thermal power is concerned (heating water) whereas scroll compressors are widespread for space heating.

Many different models of those two types of compressors with different degrees of complexity are found in the literature.

On the one hand, there are models of reciprocating compressors in which the compressor is divided in several volumes (elements such as compression chamber, valves...). Those models require input data very difficult to obtain or known only by the constructor and non-available in the data-sheets. The volumes of the different elements and the effective area of valves are also required. The transient fluid conservation equations (continuity, momentum and energy) are integrated in the whole compressor domain and the energy balance for the refrigerant inside the cylinder is computed for each time step during the operating cycle [2–7].

On the other hand, models in which thermodynamic assumptions are made are also found. In those models, data are not very difficult to obtain: e.g. refrigerant inlet state, outlet refrigerant pressure, clearance volume, motor speed. In Ref. [8] eight input data are sufficient to determine mass flow rate and required compressor power. In Refs. [9–11] (model derived from Ref. [8]) the refrigerant mass flow rate is affected by the clearance volume re-expansion, by a pressure drop in the suction valve and by a heat transfer from a fictitious isothermal wall. The friction power loss is composed of a constant contribution and another one proportional to the isentropic power. Ref. [12] presents a simple thermodynamic model for reciprocating compressors used in domestic appliances. It required the knowledge of five parameters easy to determine. The main difference between this model and the one presented in Ref. [9] is the fact that the heat transfer phenomena in the compressor are not considered in Ref. [12].

The same two categories may be defined for scroll compressors.

Models [13–16] require the knowledge of pocket volumes and perimeters for every six degrees of rotation, the height, thickness and pitch of the scrolls that are quite difficult to obtain. In those models, the whole compressor is divided in several chambers and the compression process is simulated for every gas pockets. It requires the evaluation of areas, volumes, pressures, temperatures and specific volumes for every crank angle. Mass and energy conservation equations were developed for each chamber.

Model [17] is exclusively thermodynamic and has the same philosophy as [9–11] used for reciprocating compressors. The refrigerant mass flow rate is affected by a suction temperature increase and the compression process is considered isentropic to the “adapted” pressure and isochoric until the discharge pressure.

The ARI Standard 540 [18] for positive displacement compressors recommends the use of third-degree-equations of 10 coefficients for the calculation of power input, mass flow rate of refrigerant, current or compressor efficiency. Those coefficients have no physical meaning so that the extrapolation of the performances outside the operating range used for the fitting leads to unrealistic performances values.

The purpose of this study is not the development of a complex model that can relate the performances of the compressor to its detailed geometry and that could be used for technological developments. A simple and thermodynamically realistic model is needed. It should be accurate enough to give mass flow rates and power values that can be used in a global model of a heat pump. Parameters appearing in such a model should be found in the technical datasheets of the compressors or should be determined in such a way that the calculated mass flow rate and electrical power match those given in these datasheets.

2. Reciprocating compressors

2.1. Modelling of reciprocating compressors

The model developed by Lebrun and coworkers [9–11] has been adapted given the particular requirements mentioned above.

The evolution of the thermodynamic state of the refrigerant through the compressor is presented in Fig. 1.

The compression process is divided in three steps.

- Isenthalpic pressure drop in the suction valve (i–1).
- Isobaric heating up in the suction pipe due to a heat transfer with a fictitious wall at temperature T_w (1–2).
- Isentropic compression (2–3).

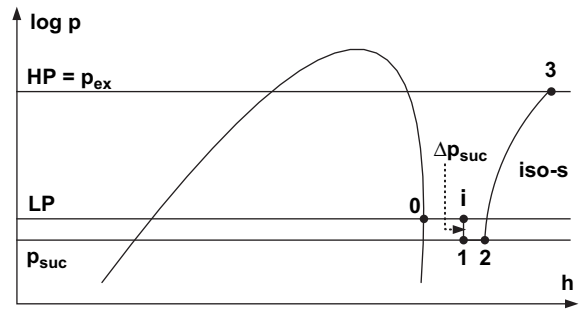


Fig. 1. Diagram ($\log p, h$) of the compression.

2.1.1. Prediction of the refrigerant mass flow rate

The data are:

- Evaporation temperature T_{evap} .
- Condensation temperature T_{cond} .
- Temperature at the compressor inlet (point i, Fig. 1) T_i or superheating ΔT_{sup} .

The parameters of the model are:

- The suction line diameter d_{suc} .
- The heat transfer coefficient multiplied by the heat transfer surface during the isobaric heating process in the suction line UA_{suc} .
- The compressor rotation speed N .
- The swept volume V_s .
- The ratio between the dead space V_d and swept volumes ε .
- The temperature of the fictitious wall T_w .

Both high and low pressures (HP and LP) can be calculated from the phase change temperatures using Ref. [19] (Refprop 7.0[®]).

$$LP = p_{\text{vsat}}(T_{\text{evap}}) \tag{1}$$

$$HP = p_{\text{vsat}}(T_{\text{cond}}) \tag{2}$$

in which $p_{\text{vsat}}(T)$ is the saturation vapour pressure law of the refrigerant.

Point 0, corresponding to the saturated vapour at low pressure (Fig. 1), is thus determined.

Temperature T_i at the inlet of the compressor (point i) is either directly given or calculated by Eq. (3).

$$T_i = T_{\text{evap}} + \Delta T_{\text{sup}} \tag{3}$$

T_i and LP allow the calculation of h_i and ρ_i respectively, the specific enthalpy and density of the refrigerant at the compressor inlet using Ref. [19].

The suction pressure p_{suc} (point 1) is given by Eq. (4).

$$p_{\text{suc}} = LP - \Delta p_{\text{suc}} \tag{4}$$

in which Δp_{suc} is the pressure drop in the suction valve; it can be deduced from Eq. (5).

$$q_m = \frac{\pi d_{\text{suc}}^2}{4} \sqrt{2\Delta p_{\text{suc}} \rho_i} \quad (5)$$

in which:

- q_m is the mass flow rate of refrigerant.
- d_{suc} is the valve coefficient considered as a pseudo dimension.

The thermodynamic state of the refrigerant at point 1 is determined by Eq. (6) using Ref. [19].

$$h_1(T_1, \text{LP}) = h_1(T_1, p_{\text{suc}}) \quad (6)$$

The temperature at the end of the isobaric heating process (transformation 1–2) T_2 may be deduced from Eq. (7).

$$UA_{\text{suc}} \Delta T_{\text{log suc}} = q_m (h_2 - h_1) \quad (7)$$

with the log-mean difference temperature defined by Eq. (8).

$$\Delta T_{\text{log suc}} = \frac{(T_w - T_1) - (T_w - T_2)}{\ln \frac{T_w - T_1}{T_w - T_2}} \quad (8)$$

In Eqs. (5) and (7), the refrigerant mass flow rate is calculated by Eq. (9).

$$q_m = \frac{1}{v_2} q_{vc} \quad (9)$$

in which:

- v_2 is the specific volume of refrigerant at point 2.
- q_{vc} is the circulated volume flow rate.

q_{vc} is determined by Eq. (10).

$$q_{vc} = V_c \frac{N}{60} \quad (10)$$

The circulated volume, V_c , is the difference between volumes V_2 and $V_{3''}$ defined in the Crank diagram (Fig. 2).

V_2 is given by Eq. (11):

$$V_2 = V_d + V_s = \varepsilon V_s + V_s \quad (11)$$

The determination of $V_{3''}$ requires the mass of gas ($m_{3''}$) and the specific volume of refrigerant ($v_{3''}$) at point 3'' (Eq. (12)).

$$V_{3''} = v_{3''} m_{3''} \quad (12)$$

Considering the expansion 3'–3'' as isentropic, the specific volume $v_{3''}$ can be calculated knowing the pressure $p_{3''}$ and the specific entropy $s_{3''}$ at point 3''.

$$p_{3''} = p_{\text{suc}} \quad (13)$$

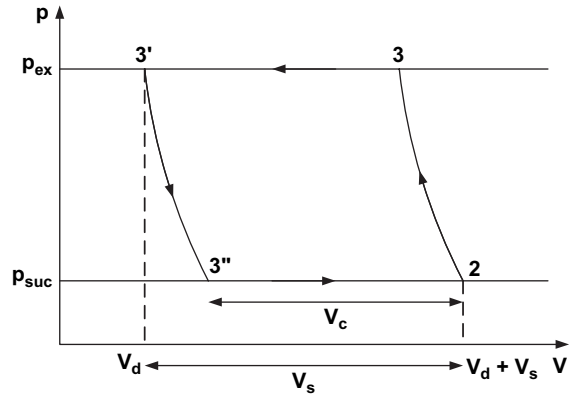


Fig. 2. Crank diagram.

$$s_{3''} = s_{3'} \quad (14)$$

$s_{3'}$ is calculated knowing the pressure $p_{3'}$ and the specific volume $v_{3'}$ at point 3'.

$$p_{3'} = \text{HP} \quad (15)$$

$$v_{3'} = v_3 \quad (16)$$

In the same way, considering the compression step as isentropic, v_3 may be calculated from pressure p_3 and specific entropy s_3 by:

$$p_3 = \text{HP} \quad (17)$$

$$s_3 = s_2 \quad (18)$$

$m_{3''}$ in Eq. (12) is calculated by:

$$m_{3''} = \frac{V_d}{v_{3'}} \quad (19)$$

Assuming that T_{evap} , T_{cond} and T_i or ΔT_{sup} are given, Eqs. (1)–(19) lead to the determination of q_m once the parameters of the model are available.

The parameters are:

- The temperature of the fictitious wall T_w .
- The heat transfer coefficient multiplied by the heat transfer surface during the isobaric heating process in the suction line UA_{suc} .
- The ratio between dead space and swept volumes ε .
- The diameter of the suction pipe d_{suc} .
- The rotation speed of the compressor N .
- The swept volume V_s .

The last two ones are given by the constructor.

The calculation procedure is given in Fig. 3.

2.1.2. Prediction of the electrical power

Once the mass flow rate is calculated, each point in Fig. 1 is known.

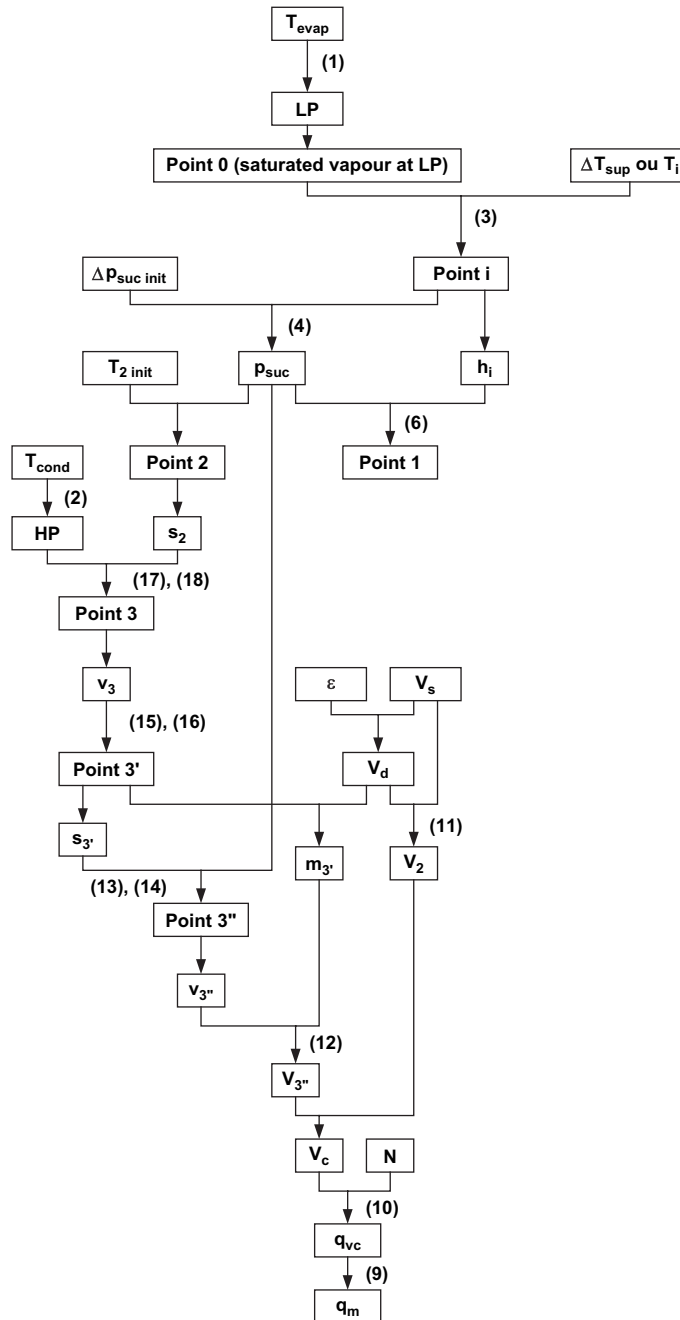


Fig. 3. Mass flow rate calculation.

In the previous section, compression (2–3) was supposed to be isentropic. The mechanical power is then written (Eq. (20)).

$$P_{mecha} = q_m(h_3 - h_2) \tag{20}$$

The calculation of the actual electric power consumption provided to the compressor requires the knowledge of the

factor ($\eta_{el}\eta_{iso-s}$), which is the product of the electrical and isentropic efficiencies.

This factor allows us to take into account both the electrical losses and the losses due to the non-isentropic compression.

This term was considered to be a polynomial function of the compression ratio (HP/LP) (Eq. (21)).

$$\eta_{el}\eta_{iso-s} = a\left(\frac{HP}{LP}\right)^6 + b\left(\frac{HP}{LP}\right)^5 + c\left(\frac{HP}{LP}\right)^4 + d\left(\frac{HP}{LP}\right)^3 + e\left(\frac{HP}{LP}\right)^2 + f\left(\frac{HP}{LP}\right) + g \quad (21)$$

Knowing the coefficients of the polynomial function it is possible to calculate the electrical power (Eq. (22)).

$$P_{elcalc} = \frac{P_{mecha}}{\eta_{iso-s}\eta_{el}} \quad (22)$$

The prediction of this power consumption requires new parameters (a, b, c, d, e, f, g) but no new operating data: HP and LP were needed for the mass flow rate calculation.

2.2. Determination of the parameters

2.2.1. Determination of the parameters: mass flow rate calculation

The four unknown parameters required for the calculation of the mass flow rate are: T_w , UA_{suc} , ε and d_{suc} . The assumption that they are constant for a given compressor and a given refrigerant is made.

Their values are found by minimizing the discrepancies between the calculated mass flow rates and the ones provided in the datasheets for given operating conditions (LP, HP, T_i , ΔT_{sup}).

The fictitious wall temperature, T_w , has not a significant influence on the mass flow rate so its value was set to 50 °C.

2.2.2. Determination of parameters: electrical power calculation

The parameters needed for the determination of the electrical power are the coefficients of the polynomial equation linking the compression ratio HP/LP to the product of efficiencies ($\eta_{el}\eta_{iso-s}$). First the isentropic mechanical power is calculated (Eq. (20)). The ratio $P_{mecha}/P_{electrical}$ is then deduced from the electrical power provided by the manufacturer in the same operating conditions.

This ratio is the product of the electrical and isentropic efficiencies ($\eta_{el}\eta_{iso-s}$) (Eq. (23)).

$$\frac{P_{mecha}}{P_{electrical}} = \eta_{iso-s}\eta_{el} \quad (23)$$

A sixth degree polynomial law is used to correlate $\eta_{el}\eta_{iso-s}$ to the compression ratio. The values of the parameters are determined by an optimization procedure.

3. Scroll compressors

3.1. Modelling of scroll compressors

The model is an adaptation of the work by Lebrun et al. [17].

The evolution of the thermodynamic state of the refrigerant through the compressor is presented in Fig. 4.

The compression process is divided in three steps.

- Isobaric heating up in the suction pipe due to a heat transfer with a fictitious wall at temperature T_w (1–2).
- First part of the compression (assumed isentropic, 2–3): the gas is compressed until the volume created by the scrolls matches exhaust volume, V_{ex} . The pressure at point 3 is called “intermediate pressure, IP”; it can be lower or greater than the high pressure.
- End of the compression at V_{ex} (constant volume) by mass accumulation in the exhaust chamber until the pressure is equal to the exhaust one (3–4).

3.1.1. Prediction of the refrigerant mass flow rate

The data are:

- Evaporation temperature T_{evap} .
- Condensation temperature T_{cond} .
- Temperature at the compressor inlet (point 1, Fig. 4) T_1 or superheating ΔT_{sup} .

The parameters of the model are:

- The temperature of the fictitious wall T_w .
- The heat transfer coefficient multiplied by the heat transfer surface during the isobaric heating process in the suction line UA_{suc} .
- The swept volume V_s .
- The compressor rotation speed N .

Both high and low pressures (HP and LP) can be calculated from the phase change temperatures using Ref. [19].

$$LP = p_{vsat}(T_{evap}) \quad (24)$$

$$HP = p_{vsat}(T_{cond}) \quad (25)$$

in which $p_{vsat}(T)$ is the saturation vapour pressure law of the refrigerant.

Point 0, corresponding to the saturated vapour at low pressure (see Fig. 4), is thus determined.

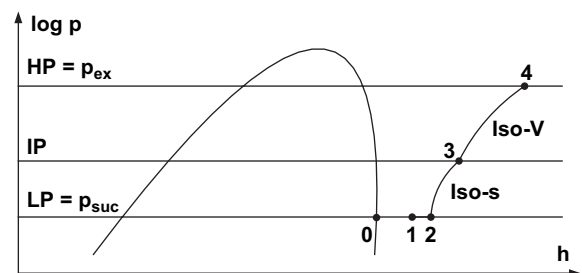


Fig. 4. Diagram ($\log p, h$) of the thermodynamic process.

Temperature T_1 at the inlet of the compressor (point 1) is either directly given or calculated by Eq. (26).

$$T_1 = T_{\text{evap}} + \Delta T_{\text{sup}} \quad (26)$$

T_1 and LP allow the calculation of h_1 , specific enthalpy of the refrigerant at the compressor inlet using Ref. [19].

The temperature at the end of the isobaric heating process (transformation 1–2) T_2 may be deduced from Eq. (27).

$$UA_{\text{suc}} \Delta T_{\text{log suc}} = q_m (h_2 - h_1) \quad (27)$$

in which q_m is the mass flow rate of refrigerant.

With the log-mean difference temperature defined by Eq. (28).

$$\Delta T_{\text{log suc}} = \frac{(T_w - T_1) - (T_w - T_2)}{\ln \frac{T_w - T_1}{T_w - T_2}} \quad (28)$$

In Eq. (27), the refrigerant mass flow rate is calculated by Eq. (29).

$$q_m = \frac{1}{v_2} V_s N \quad (29)$$

in which v_2 is the specific volume of refrigerant at point 2.

Assuming T_{evap} , T_{cond} and T_1 or ΔT_{sup} are given, Eqs. (24)–(29) lead to the determination of q_m once the parameters of the model are available.

The parameters are:

- The temperature of the fictitious wall T_w .
- The heat transfer coefficient multiplied by the heat transfer surface during the isobaric heating process in the suction line UA_{suc} .
- The swept volume V_s .
- The rotation speed of the compressor N .

The last two ones are given by the constructor.

The calculation procedure is given in Fig. 5.

3.1.2. Prediction of the electrical power

The compression 2–3 is supposed to be isentropic. It occurs between the low pressure and the intermediate pressure for which the exhaust volume is obtained. This intermediate

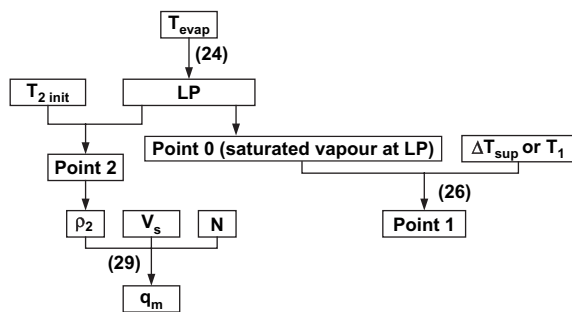


Fig. 5. Mass flow rate calculation.

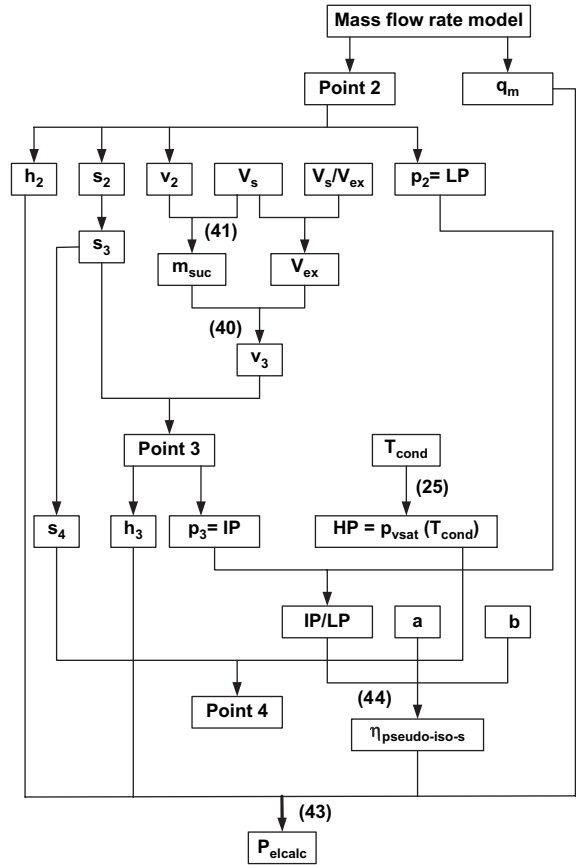


Fig. 6. Determination of power consumption, diagram.

pressure, IP, can be either higher or lower than the high pressure.

The mechanical work W_{23} corresponding to this compression step is given by Eq. (30).

$$W_{23} = m_{\text{suc}} (u_3 - u_2) \quad (30)$$

in which:

- u is the specific internal energy of the gas.
- m_{suc} is the suctioned mass.

Table 1
Characteristics of the studied reciprocating compressors

Compressor	Volumic flow rate ($\text{m}^3 \text{h}^{-1}$)	Number of cylinders	Bore (mm)	Stroke (mm)	P (W) (R134a, $T_{\text{cond}} = 40^\circ\text{C}$, $T_{\text{evap}} = 0^\circ\text{C}$)
R1	39.36	4	60	40	5080
R2	73.6	4	70	55	9460
R3	55.99	4	63.5	50.8	7600
R4	70.9	4	68.3	55.6	9150
R5	14.9	2	Not available	Not available	2162

Table 2
Reciprocating compressors: results

Compressor	Fluid	UA _{suc} (W K ⁻¹)	d _{suc} (cm)	ε (%)	Discrepancy q _m (%)	Discrepancy P (%)
Compressor R1: V _s = 452.414 cm ³ , N = 1450 t min ⁻¹	R134a	43.53	2.918	2.50	1.04	3.45
	R404A	48.46	1.772	2.36	0.99	2.37
	R22	48.91	2.275	4.24	1.02	2.71
	R12	50	2.457	4.22	1.11	1.66
Compressor R2: V _s = 845.977 cm ³ , N = 1450 t min ⁻¹	R134a	15.66	2.781	3.41	0.53	1.30
	R404A	19.01	2.043	2.97	0.34	1.16
	R22	19.77	2.405	4.28	0.50	2.30
	R12	20.35	2.567	4.18	1.42	0.53
Compressor R3: V _s = 643.563 cm ³ , N = 1450 t min ⁻¹	R134a	67.93	2.610	4.73	0.80	1.98
	R404A	40.09	2.105	4.59	0.75	1.45
	R22	5.35	1.962	5.91	0.37	2.24
Compressor R4: V _s = 814.943 cm ³ , N = 1450 t min ⁻¹	R134a	104.39	3.417	5.11	1.22	1.24
	R404A	95.44	2.678	4.79	1.09	0.86
	R22	43.97	2.432	5.88	0.39	0.82
Compressor R5: V _s = 85.64 cm ³ , N = 2900 t min ⁻¹	R134a	13.77	1.221	8.25	1.86	2.79
	R404A	19.38	1.017	6.76	3.06	1.65
	R407C	22.18	1.132	8.55	1.59	1.23

The mechanical work during suction, W_{suc}, is given by Eq. (31).

$$W_{suc} = -V_{suc}LP \tag{31}$$

The work at the exhaust, W_{ex}, is given by Eq. (32).

$$W_{ex} = V_{ex}HP \tag{32}$$

The total work between points 2 and 4 is obtained by the summation of the three works (relations (30)–(32)).

Volumes V_{suc} and V_{ex} can also be written as Eqs. (33) and (34).

$$V_{suc} = m_{suc}v_2 \tag{33}$$

$$V_{ex} = m_{suc}v_3 \tag{34}$$

which leads to Eq. (35).

$$W = m_{suc}(u_3 - u_2) - LPm_{suc}v_2 + HPm_{suc}v_3 \tag{35}$$

given

$$u_2 = h_2 - LPv_2 \tag{36}$$

$$u_3 = h_3 - IPv_3 \tag{37}$$

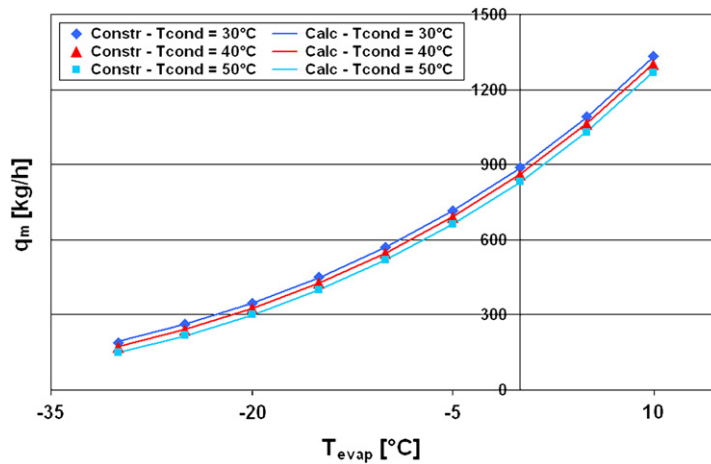


Fig. 7. Compressor R2, R134a – q_m = f(T_{evap}).

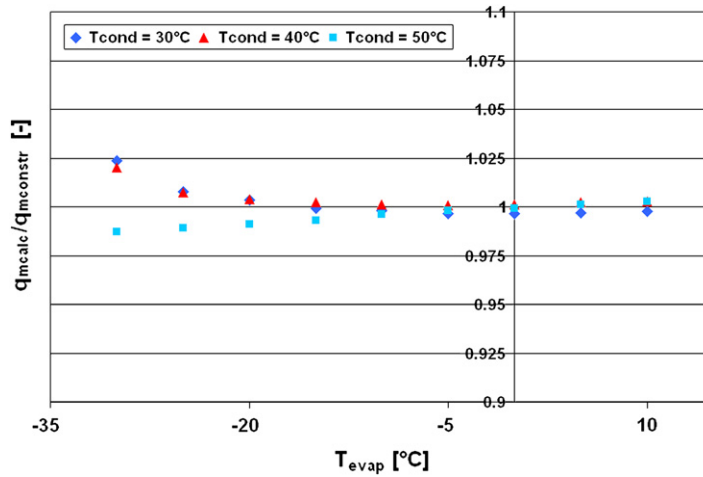


Fig. 8. Compressor R2, R134a – $q_{mcalc}/q_{mconstr} = f(T_{evap})$.

Eq. (35) becomes Eq. (38).

$$W = m_{suc}(h_3 - h_2) + (HP - IP)m_{suc}v_3 \quad (38)$$

which leads to the expression of the power (Eq. (39)).

$$P = q_m(h_3 - h_2) + (HP - IP)q_mv_3 \quad (39)$$

In Eq. (39) q_m is determined by the procedure described in Section 3.1.1; h_2 is calculated by Ref. [19] knowing the temperature and pressure conditions at point 2; the high pressure HP is known via relation (24).

The specific volume v_3 is calculated by:

$$v_3 = \frac{V_{ex}}{m_{suc}} \quad (40)$$

in which:

- The exhaust volume V_{ex} is determined from the suction volume (given by the constructor) and from the ratio between this volume and the exhaust volume (V_{suc}/V_{ex}) which is a parameter of the model.
- The suctioned mass m_{suc} is calculated by:

$$m_{suc} = \frac{V_{suc}}{v_2} \quad (41)$$

with v_2 calculated by Ref. [19].

In Eq. (39), point 3 (h_3 and IP) is known because both the specific volume v_3 and the specific entropy s_3 are known (Eqs. (40) and (42)).

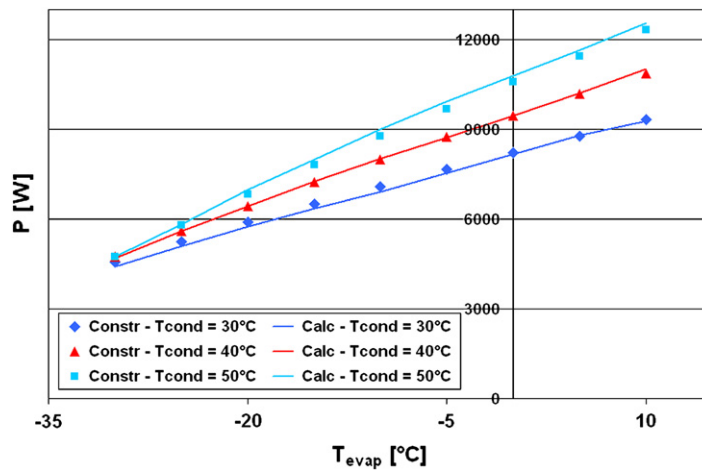


Fig. 9. Compressor R2, R134a – $P = f(T_{evap})$.

$$s_3 = s_2 \tag{42}$$

Knowing each term in relation (39), it is possible to calculate P which is the thermodynamic mechanical power (with the first step considered as isentropic). The calculation of the electrical power P_{elcalc} would require the introduction of an isentropic efficiency in the first term of the right-hand member of Eq. (39) as well as an electrical efficiency applied to each step of the compression. Due to the fact that these two efficiencies are not applied to the same terms it is not possible to gather them in one term ($\eta_{el}\eta_{iso-s}$) as it was the case for reciprocating compressors. It appeared that the introduction of two new parameters to be dealt with in the optimization procedure led to unrealistic parameter values and to too good performances compared to the experimental accuracy of the data. As a consequence, given the low influence of the second term of the right-hand term of Eq. (39), we only introduced one parameter (applied to the isentropic step) called the pseudo-isentropic efficiency and which takes into account both the irreversibilities and the electrical losses.

$$P_{elcalc} = \frac{q_m(h_3 - h_2)}{\eta_{pseudo-iso-s}} + (HP - IP)q_m v_{3real} \tag{43}$$

For a correct representation of the electrical power, it appeared that this pseudo-isentropic efficiency should be considered as a linear function of the ratio IP/LP. v_{3real} is the specific volume at the “real” point 3 (non-isentropic).

The power calculation procedure is presented in Fig. 6.

3.2. Determination of the parameters

3.2.1. Determination of the parameters: mass flow rate calculation

The two unknown parameters in the mass flow rate prediction are T_w and UA_{suc} . The assumption that they are constant for a given compressor and a given refrigerant is made.

Their values are found by minimizing the discrepancies between the calculated mass flow rates and the ones provided in the datasheets for given operating conditions.

The fictitious wall temperature, T_w , has no significant influence on the mass flow rate so that its value was set to 50 °C.

3.2.2. Determination of the parameters: electrical power calculation

The influent parameters in the power prediction are the ratio between the suction and the exhaust volumes (V_{suc}/V_{ex}) and the coefficients of the linear law of the pseudo-isentropic efficiency ($\eta_{pseudo-iso-s}$) versus the compression ratio IP/LP.

The isentropic efficiency is expressed by Eq. (44).

$$\eta_{pseudo-iso-s} = a \frac{IP}{LP} + b \tag{44}$$

These three parameters are determined by minimizing the discrepancies between the calculated electrical power and the ones provided in the datasheets for given operating conditions.

4. Results

In this section, simulation results of mass flow rate and power for both types of compressors are presented.

4.1. Reciprocating compressors

Five reciprocating compressors were studied. Some of their characteristics are presented in Table 1 [20–22].

Table 2 presents values of the different parameters (UA_{suc} , d_{suc} and ϵ) and the average discrepancies, respectively, on the mass flow rate and on the electrical power for each compressor and each studied fluid.

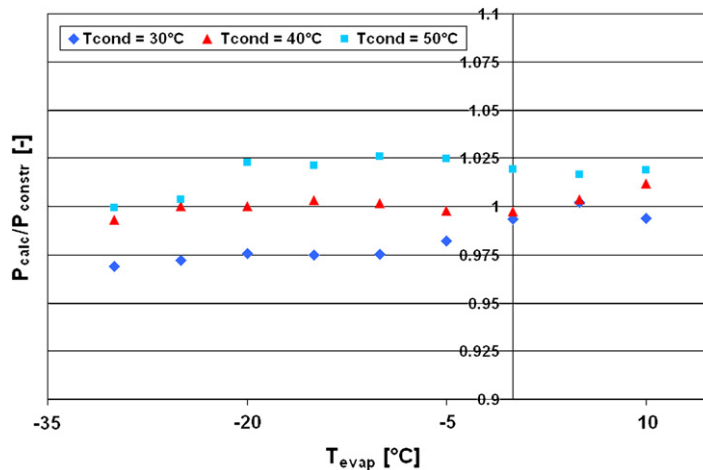


Fig. 10. Compressor R2, R134a – $P_{calc}/P_{const} = f(T_{evap})$.

Table 3
Characteristics of the studied scroll compressors

Compressor	Volumic flow rate ($\text{m}^3 \text{h}^{-1}$)	P (W) (R134a, $T_{\text{cond}} = 40^\circ\text{C}$, $T_{\text{evap}} = 0^\circ\text{C}$)
S1	25	3770
S2	36	5420
S3	8.6	1340
S4	35.56	5500
S5	43.5	6866

The model is very good at predicting mass flow rate and power consumption of reciprocating compressors: average discrepancies are lower than 3%. In most cases, the points for which the discrepancy is higher than 5% correspond to evaporation temperatures lower than -20°C and/or condensation temperature higher than 60°C . In residential heat pumps, those ranges of temperatures are rare.

Figs. 7 and 8 present, respectively, the evolution of the mass flow rate (calculated and given by the manufacturer) and the related discrepancy as a function of the evaporation temperature for different condensation temperatures (30, 40 and 50°C).

For evaporation temperatures higher than -20°C the discrepancy on the mass flow rate is lower than 1%.

Figs. 9 and 10 present, respectively, the evolution of the electrical power (calculated and given by the manufacturer) and the related discrepancy as a function of the evaporation temperature for different condensation temperatures (30, 40 and 50°C).

For evaporation temperatures higher than -20°C the discrepancy on the mass flow rate is lower than 2.5%.

4.2. Scroll compressors

Five reciprocating compressors were studied. Some of their characteristics are presented in Table 3 [20–22].

Table 4 presents the values of the different parameters (UA_{suc} , $V_{\text{suc}}/V_{\text{ex}}$, a and b) and the average discrepancies, respectively, on the mass flow rates and on the electrical powers for each compressor and each fluid.

The model is very good at predicting mass flow rate and power of scroll compressors. The mean discrepancies are lower than 3.5%. In most cases, points for which discrepancy is higher than 5% correspond to evaporation temperatures lower than -20°C and/or condensation temperature higher than 60°C . In the residential heat pumps, those ranges of temperatures are rare.

Figs. 11 and 12 present, respectively, the evolution of mass flow rate and the discrepancy on this mass flow rate as a function of the evaporation temperature for different condensation temperatures.

The discrepancy on the mass flow rate is generally lower than 5%. It can reach nearly 10% for high condensation temperatures (55 and 60°C).

Figs. 13 and 14 present, respectively, the evolution of power and the discrepancy on this power as a function of the evaporation temperature for different condensation temperatures.

Table 4
Scroll compressors: results

Compressor	Fluid	UA_{suc} (W K^{-1})	$V_{\text{suc}}/V_{\text{ex}}$ (–)	a (–)	b (–)	Discrepancy q_m (%)	Discrepancy P (%)
Compressor S1: $V_s = 143.678 \text{ cm}^3$, $N = 2900 \text{ t min}^{-1}$	R134a	19.01	2.379	–0.777	2.585	1.70	1.12
	R404A	48.36	2.165	0.010	0.682	1.57	0.19
	R407C	42.06	2.219	–0.312	1.463	2.31	0.46
	R22	60.33	2.187	–0.671	2.329	2.21	0.59
Compressor S2: $V_s = 206.897 \text{ cm}^3$, $N = 2900 \text{ t min}^{-1}$	R134a	26.99	2.378	–0.772	2.570	1.74	1.12
	R404A	69.59	2.166	0.003	0.698	1.59	0.16
	R407C	59.49	2.220	–0.316	1.473	2.31	0.46
	R22	87.09	2.189	–0.677	2.345	2.18	0.59
Compressor S3: $V_s = 47.778 \text{ cm}^3$, $N = 3000 \text{ t min}^{-1}$	R134a	5.39	2.302	–0.473	1.766	1.47	0.85
	R404A	18.97	2.089	–0.320	1.361	2.95	1.02
	R22	22.67	2.128	–0.642	2.142	3.15	2.26
	R407C	17.44	2.156	–1.152	3.302	1.97	1.21
Compressor S4: $V_s = 197.556 \text{ cm}^3$, $N = 3000 \text{ t min}^{-1}$	R134a	107.02	2.637	–0.134	1.022	2.32	0.53
	R404A	44.93	2.667	–0.113	0.954	2.95	1.49
	R22	131.05	2.937	–0.215	1.422	2.78	1.24
	R407C	146.36	2.799	–0.194	1.273	2.95	1.08
Compressor S5: $V_s = 24.99 \text{ cm}^3$, $N = 2900 \text{ t min}^{-1}$	R134a	34.64	2.466	–0.826	2.752	2.02	0.66
	R22	62.43	2.293	–0.579	2.148	1.84	0.58
	R407C	99.14	2.239	–0.465	1.787	2.23	0.55

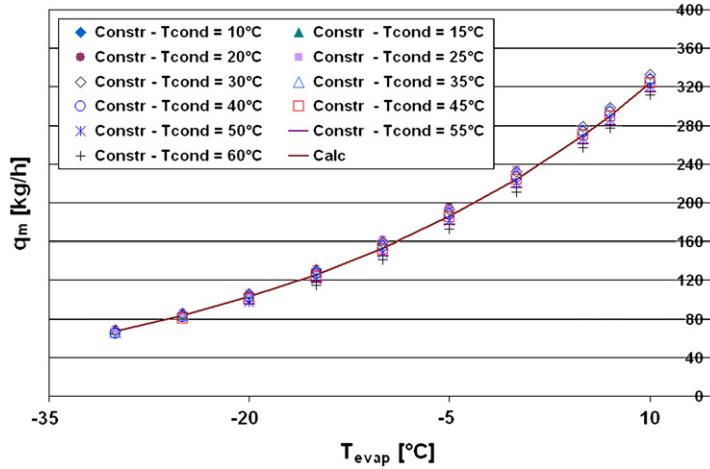


Fig. 11. Compressor S3, R404A – $q_m = f(T_{evap})$.

The discrepancy on the power is also generally lower than 5%. It can be higher than 5% for low condensation temperatures (10 and 15 °C).

5. Conclusion

In this paper, simple and thermodynamically realistic models of the two types of compressors found in the residential heat pumps (reciprocating and scroll compressors) have been presented. Those models calculate the mass flow rate of refrigerant and the power consumption from the knowledge of operating conditions (phase change temperatures and refrigerant temperature at the inlet of the compressor or superheating) and different parameters.

Parameters appearing in the models are found in the technical datasheets of the compressors or they are fitted in such a way that the calculated mass flow rate and electrical power match those given in these datasheets.

The reciprocating compressor model requires the knowledge of six parameters. Two of them are given in the datasheets: the swept volume (V_s) and the compressor rotation speed (N). The last four are: the temperature of the fictitious wall (T_w) which is actually set to a constant value (50 °C), the global heat transfer coefficient at suction (UA_{suc}), the diameter of the suction pipe (d_{suc}) and the ratio between the dead space and the swept volume (ϵ). Those three parameters have to be fitted in order that the calculated mass flow rates match the ones given in the datasheets. The determination of the powers requires the knowledge of the seven coefficients of the polynomial law relating the product of the electrical and isentropic efficiencies to the compression ratio.

This model has been tested on five compressors. The mean discrepancies values on the determination of, respectively, mass flow rate and power consumption are 1.15 and 2.04% (R134a), 1.38 and 1.43% (R404A),

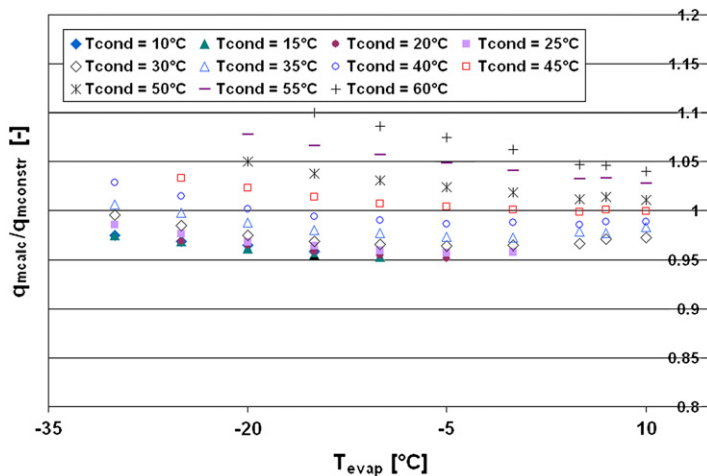


Fig. 12. Compressor S3, R404A – $q_{mcalc}/q_{mconstr} = f(T_{evap})$.

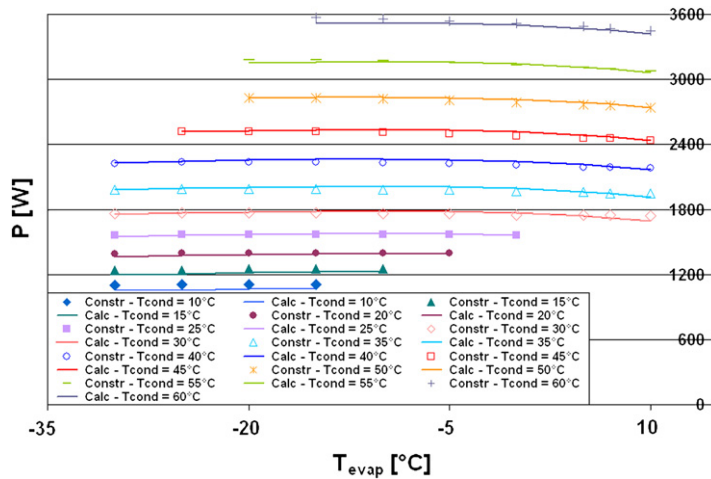


Fig. 13. Compressor S3, R404A – $P = f(T_{evap})$.

0.51 and 1.86% (R22), 1.27 and 1.09% (R12), 1.59 and 1.23% (R407C).

The scroll compressor model requires the knowledge of seven parameters. Two of them are given in the datasheets: the swept volume (V_s) and the compressor rotation speed (N). The last five are: the temperature of the fictitious wall (T_w) which is actually set to a constant value (50 °C), the global heat transfer coefficient at suction (UA_{suc}), the ratio between the swept volume and the exhaust volume (V_{suc}/V_{ex}) and the two parameters a and b of the linear law of the pseudo-isentropic efficiency. Those four parameters have to be fitted in order that the calculated mass flow rate and power matches those given in the datasheets. UA_{suc} is fitted using the mass flow rate data while the three other parameters (V_{suc}/V_{ex} , a , and b) are fitted using power consumption data.

This model has been tested on five compressors. The mean discrepancy values on mass flow rate and power are 1.89 and 0.76% (R134a), 2.76 and 1.12% (R404A), 2.39 and 0.91% (R407C), 2.59 and 1.31% (R22).

Although, it was not hinted in this paper those models fail at predicting correct outlet temperatures (up to 50 °C difference depending on the compressor and fluid, usually the difference is around 20–25 °C). So the same philosophy at the outlet than at the inlet (taking into account a heat transfer with the fictitious wall) should be applied. The determination of the global heat transfer coefficient at the exhaust (UA_{ex}) requires values of exhaust temperature or values of heat flow rate at the condenser. As temperature T_w has a significant influence on the outlet temperature of the compressor, it seems interesting to make it vary with the phase change temperatures and power consumption of the compressor.

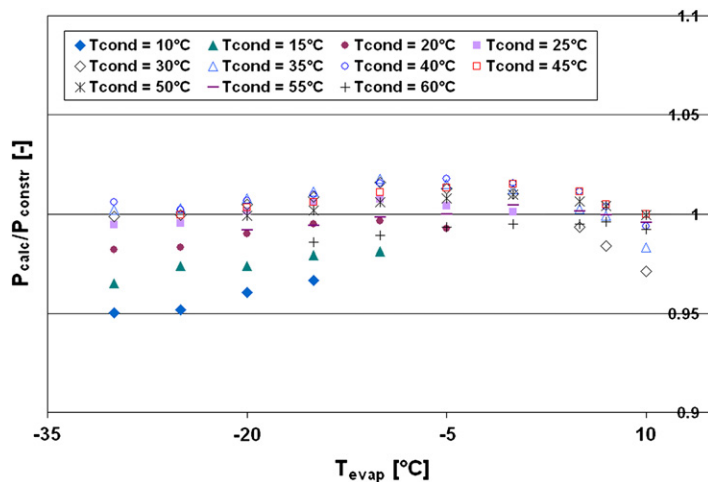


Fig. 14. Compressor S3, R404A – $P_{calc}/P_{constr} = f(T_{evap})$.

It is also possible to determine one set of parameters for all the refrigerants and for a given compressor.

It must also be noticed that the isentropic and electrical efficiencies that are used for the determination of the power have no real physical sense (the use of parameters with physical sense leads to an over-parameterised model). This lack of physical sense can explain the higher discrepancies at high temperatures.

References

- [1] H. Rivoalen, Heat Pump Market Overview in Europe, Hands-on Experience with Heat Pumps in Buildings, Workshop Report HPC-WR-23, Arnhem, The Netherlands, October 2001.
- [2] C.D. Pérez-Segarra, J. Rigola, A. Oliva, Modelling and numerical simulation of the thermal and fluid dynamic behaviour of hermetic reciprocating compressors. Part 1: theoretical basis, *HVAC & R Research* 9 (2) (2003) 215–235.
- [3] J. Rigola, C.D. Pérez-Segarra, A. Oliva, Modelling and numerical simulation of the thermal and fluid dynamic behaviour of hermetic reciprocating compressors. Part 2: experimental investigation, *HVAC & R Research* 9 (2) (2003) 237–249.
- [4] J. Rigola, C.D. Pérez-Segarra, A. Oliva, Parametric studies on hermetic reciprocating compressors, *International Journal of Refrigeration* 28 (2005) 253–266.
- [5] J. Rigola, C.D. Pérez-Segarra, A. Oliva, J.M. Serra, M. Escribà, J. Pons, Advanced numerical simulation model of hermetic reciprocating compressors, Parametric study and detailed experimental validation, in: *Proceedings of the 15th International Compressor Engineering Conference at Purdue University, USA, 2000*, pp. 23–30.
- [6] J.M. Corberán, J. González, J. Urchueguía, A. Calás, Modelling of refrigeration compressors, in: *Proceedings of the 15th International Compressor Engineering Conference at Purdue University, USA, 2000*, pp. 571–578.
- [7] M.L. Todescat, F. Fagotti, Thermal energy analysis in reciprocating hermetic compressors, in: *Proceedings of the International Compressor Engineering Conference at Purdue University, USA, 1992*, pp. 1419–1428.
- [8] P. Popovic, H.N. Shapiro, A semi-empirical method for modelling a reciprocating compressor in refrigeration systems, *ASHRAE Transactions* 101 (1995) 367–382.
- [9] E. Winandy, O.C. Saavedra, J. Lebrun, Simplified modelling of an open-type reciprocating compressor, *International Journal of Thermal Science* 41 (2002) 183–192.
- [10] M. Grodent, J. Lebrun, E. Winandy, Simplified modelling of an open-type reciprocating compressor using refrigerants R22 et R410A. 2nd part: model, in: *Proceedings of the 20th International Congress of Refrigeration, Sidney, vol. 3, 1999* (paper 800).
- [11] C. Hannay, J. Lebrun, D. Negoiu, E. Winandy, Simplified modelling of an open-type reciprocating compressor using refrigerants R22 et R410A. 1st part: experimental analysis, in: *Proceedings of the 20th International Congress of Refrigeration, Sidney, vol. 3, 1999* (paper 657).
- [12] D.I. Jähnig, D.T. Reindl, S.A. Klein, A semi-empirical method for representing domestic refrigerator/freezer compressor calorimeter test data, *ASHRAE Transactions* 106 (2000) 122–130.
- [13] J.-L. Caillat, S. Ni, M. Daniels, A computer model for scroll compressors, in: *Proceedings of the International Compressor Engineering Conference at Purdue University, USA, 1988*, pp. 47–55.
- [14] Y. Chen, N.P. Halm, E.A. Groll, J.E. Braun, Mathematical modelling of scroll compressors. Part I: compression process modelling, *International Journal of Refrigeration* 25 (2002) 731–750.
- [15] Y. Chen, N.P. Halm, E.A. Groll, J.E. Braun, Mathematical modelling of scroll compressors. Part II: overall scroll compressor modelling, *International Journal of Refrigeration* 25 (2002) 751–764.
- [16] C. Shein, R. Radermacher, Scroll compressor simulation model, *Journal of Engineering for Gas Turbines and Power* 123 (2001) 217–225.
- [17] E. Winandy, O.C. Saavedra, J. Lebrun, Experimental analysis and simplified modelling of a hermetic scroll refrigeration compressor, *Applied Thermal Engineering* 22 (2002) 107–120.
- [18] Performance Rating of Positive Displacement Refrigerant Compressors and Compressor Units, ARI Standard 504, Air-Conditioning and Refrigeration Institute, Arlington, 2004.
- [19] REFPROP, NIST Standard Reference Database 23, Version 7.0.
- [20] Bitzer – Software, <<http://www.bitzer.de>>.
- [21] Copeland Selection Software Select, <<http://www.ecopeland.com>>.
- [22] Products datasheets, <<http://danfoss.com>>.